International Journal of Mechanics and Energy (IJME)
Vol. 13, Issue 1, 2026, ISSN: 2286-5845

Hybrid FEM–PINN (MDR) Approach for Analyzing Assembly Variations with Micro-Geometric Defects

Ali Radhouan*, Maroua Ghali, Nizar Aifaoui

Mechanical Engineering Laboratory, National Engineering School of Monastir (LGM-ENIM), University of Monastir, 5 Av. Ibn Eljazzar,5019, Monastir, TUNISIA

Abstract: An analysis of geometric defects in plate assembly under linear-elastic conditions is investigated. A hybrid FEM–PINN (MDR) model is proposed, combining the finite element method, the analytical dimensionality reduction method, and physics-informed neural networks. This approach enables the coupling of physics-based modeling with data-driven learning. PINNs explicitly incorporate governing physical laws, including constitutive relations and contact conditions, into the training process using the dimensionality reduction method solutions, thereby ensuring the physical consistency of the predicted responses. This integration provides a trade-off between high-fidelity numerical modeling and reduced computational complexity. Additionally, the use of machine learning enhances computational efficiency while maintaining robustness, accuracy, and reliability in analyzing mechanical assemblies. The methodology is validated through a case study of a simple linear-elastic component assembly, and the results are given and discussed to demonstrate its effectiveness.

Key words: Flexible assembly, Fem, Physics neural networks, Dimensionality reduction.

1. Introduction

In industry, controlling assembly variation is essential for improving production processes [1]. Assemblies are generally classified into two categories: rigid assemblies, which assume infinitely rigid components, and flexible assemblies, such as those involving thin plates, which present greater complexity [2,3]. For the latter, simultaneously accounting for part flexibility and geometric defects is essential, as these factors directly affect structural behavior, simulation accuracy and reliability of the assembly [4,5]. When two components are joined, the contact problem needs to be considered.

1.1 Contact between two elastic parts

In the assembly of mechanical parts, it is essential to analyze the functional contact surfaces to ensure proper mechanical performance and structural behavior of the overall assembly. In literature, numerous models and formulations have been developed to address contact problems, where nonlinearities such as friction are incorporated in both static and dynamic cases. Computational costs and convergence challenges can motivate alternative or hybrid modeling strategies. Fig.1 illustrates the contact between two deformable bodies S^i (i = 1,2), initially occupying the domains Ω_i oriented by their normal n_i and, in their deformed configuration, the domains Ω_t^i [6,7].

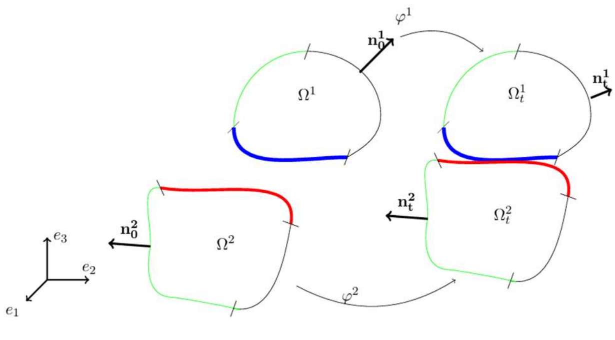

Fig.1 Schematic of objects in contact

* **Corresponding author:** Ali Radhouan
E-mail: ali.radhouan@gmail.com

For a point $x \in \Omega^i$ is associated a point $y = Y(x,t)$ in new contact through a transformation T defined by (1):

$$T = \nabla_x Y(x,t) \quad (1)$$

In this paper, for the sake of simplicity, the analysis is restricted to static conditions, with emphasis on linear elastic problems under frictionless normal contact. The contact problem is treated using a semi-numerical model based on dimensionality reduction, in which micro-defects are incorporated.

1.2 General Concept of the MDR Method

The Method of Dimensionality Reduction (MDR), introduced by Popov [8,9], simplifies 3D contact problems by mapping them onto equivalent 1D spring systems. Assuming linear elasticity and homogeneous materials, MDR provides exact, and validated solutions for a variety of geometries, particularly for frictionless axisymmetric normal contact. Thus, significantly reducing computational complexity. Fig.2 illustrates an equivalent 1D of the 3D contact problem under linear elastic assumptions.

Thus, the contact problem can be equivalent to the contact of a rigid indenter with a 3D profile F(r), where r is the polar radius in the contact plane.

The stiffness of each spring is defined by (2):

$$\Delta k_z = E^* \Delta x \quad (2)$$

The contribution of a single x coordinate spring to the normal force is then defined by (3):

$$\mathrm{F(r)} = \frac{2}{\pi}\int_0^r \mathrm{G(x)} \frac{dx}{\sqrt{(r^2 - x^2)}} \quad (3)$$

Where $\mathrm{G(x)}$ is 1D profile.

The boundaries conditions are written as in (4):

$$\begin{cases} w(r) = d - F(r), \; r \le a \\ \sigma_{zz}(r) = 0, \; r > a \end{cases} \quad (4)$$

where a is the contact radius.

Indeed, the normal displacement $w(r)$ can be defined for IN and Out contact area, nevertheless normal stress $\sigma_{zz}(r)$ is equal to zero outside the contact zone [8].

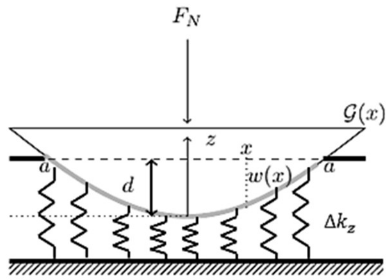

Fig.2 Equivalent 1D problem of the 3D contact problem under the linear elastic axisymmetric case

The remainder of this paper is organized as follows. Section 2 introduces the problem description and formulation of the PINN model. Section 3 presents the results and discussion, highlighting the effectiveness of the proposed approach. Finally, Section 4 provides the main conclusions and perspectives.

2. Problem description and proposed model

The problem consists of evaluating the assembly variation of two steel plates (E_1=207000 MPa;$\upsilon_1 = 0.3$;E_2 =220000MPa; $\upsilon_2 = 0.3$ 4); modeled as isotropic homogeneous materials, while incorporating micro-geometric defects represented by a cosine function with amplitude $A \in [-0.001, 0.001]$ [10]. Plate 2 is slightly more rigid than plate 1 since it represents the indenter in the MDR model. The plates with dimensions of $400 \times 200\ mm$, are joined with 8 mm diameter titanium bolts (03) (Fig.3a) and clamped at their ends. A vertical load of 67 N is first applied to allow bolts insertion, after which the bolts are locked to secure the assembly. To solve this problem, a hybrid FEM-PINN(MDR) framework is adopted under linear elastic and frictionless contact conditions as shown in Fig.4. Here, $q_i^{MDR}(x)$ represents the pression distribution along the contact interface.

Under the assumption of small deformations and considering defects at the microscale, the approach adopts a two-level analysis: a macro-scale FEM to capture global stiffness and displacements, and a micro-scale PINN–MDR to account for defect-sensitive contact behavior. In each analysis different meshes $\Omega_i^h \equiv \Omega_{i1}^h \cup \Omega_{i2}^h$ are adopted (Fig.3b), where Γ_c is the contact zone with dimensions 40x200 mm^2.

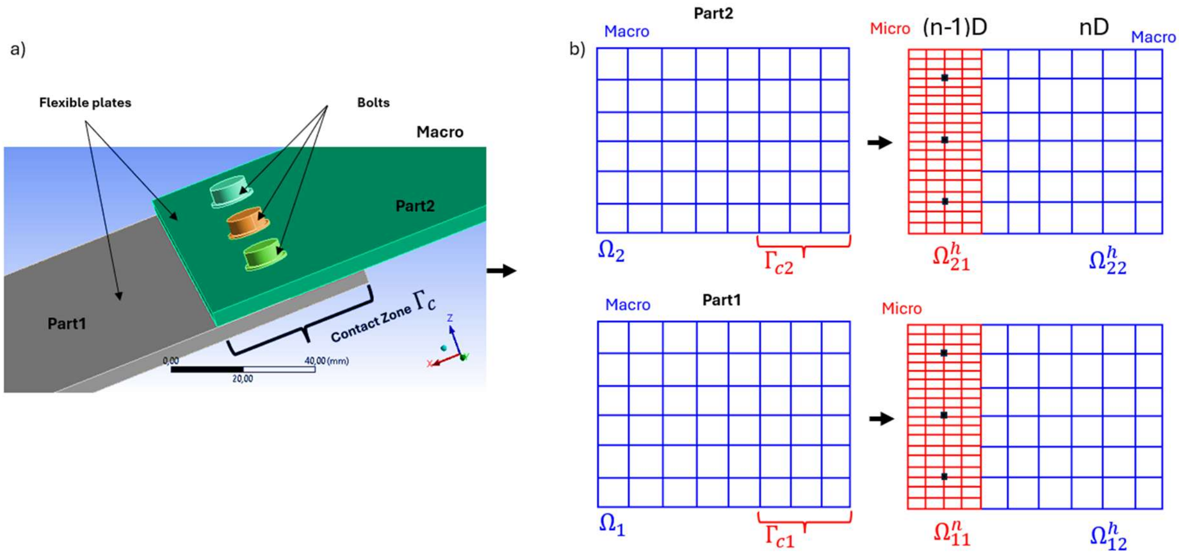

Fig.3 Flexible assembly: a) simplified plate assembly process; b) mesh of subdomains (macro and micro levels)

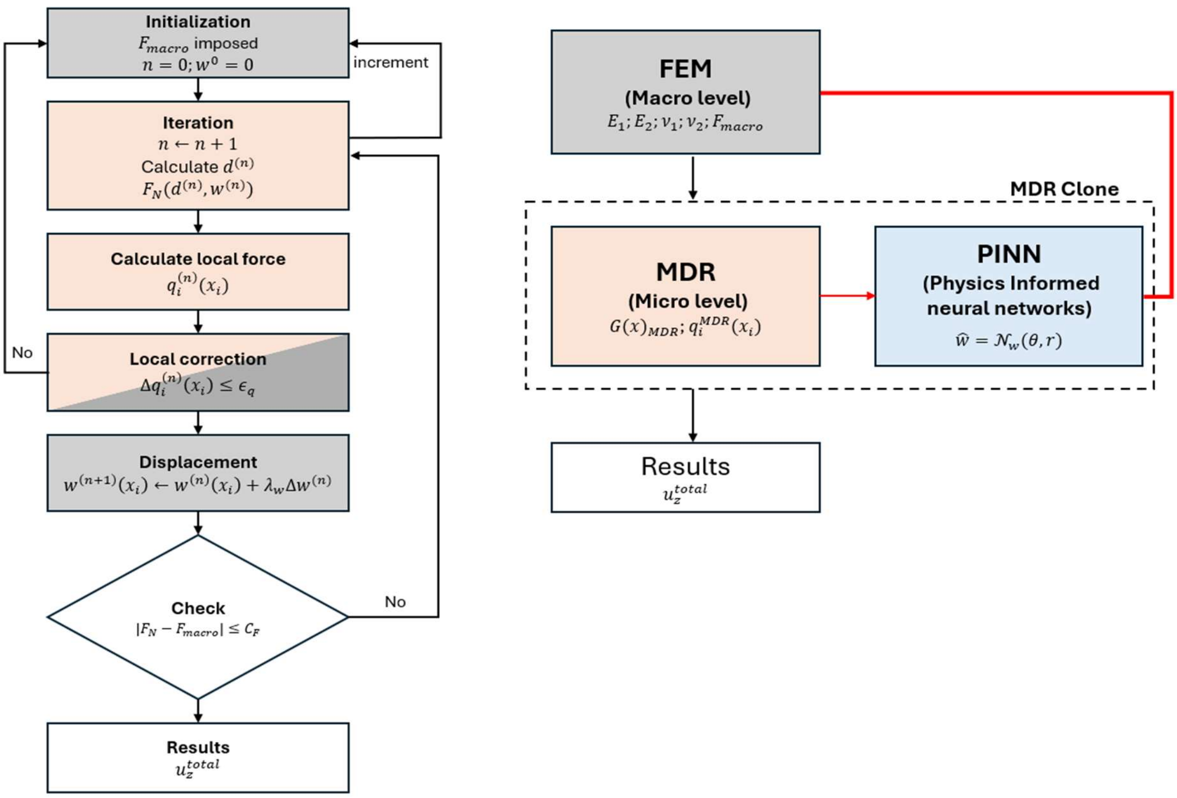

Fig.4 Flowchart of the FEM-PINN(MDR) model

The amplitude A directly determines the intensity of the geometric variation associated with the micro-defect along the normal direction to the nominal surface. It therefore governs the magnitude of the

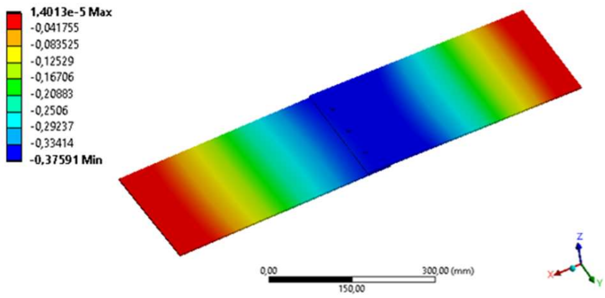

Fig.5 Simulation of assembly variation showing the global normal displacement along Z-axis

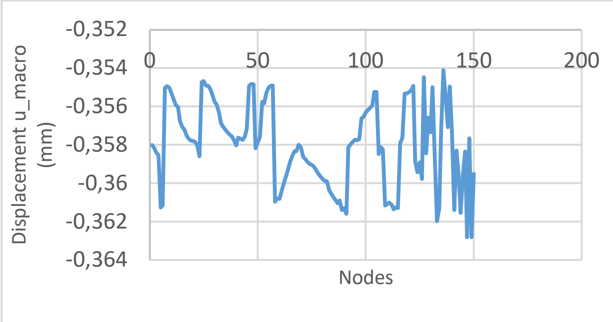

Fig.6 Nodal displacement for the first 150 selected nodes

normal displacements u_z^{micro}, which represents the local deviation from the reference geometry.

In practice, typical surface conditions specified according to ISO 21920 exhibit arithmetic mean roughness values generally ranging from $R_a = 0.8\,\mu m$ to $R_a = 3.2\,\mu m$, particularly for steel plate surfaces. In this context, an amplitude on the order of $A \approx 5\,\mu m$ can be considered to represent a relatively rough surface condition, while remaining consistent with standardized industrial specifications.

For sake of simplicity, some assumptions are introduced in this work, and the problem is simplified under the small-deformation assumption, frictionless normal contact, where the dimensionality reduction method (MDR) 1D is applied. The main objective is to employ physics-informed neural networks (PINNs), trained using the exact MDR solutions, as illustrated in Fig.4. The main steps of this approach, which involve a Macro–Micro analysis, are presented in the following section.

2.1 FEM model

For a flexible component, the geometric and mechanical states are related by (5):

$$F = \mathbb{K}\, u \tag{5}$$

Where F is the applied force vector, u is the displacement vector, and $\mathbb{K}$ is the stiffness matrix, dependent on material properties and geometry under small deformations. Elastic responses can be expressed either as forces for imposed displacements model or as displacements for imposed forces, accounting for bending effects. Fig.5 presents the assembly simulation using the FEM approach with a coarse mesh.

In this work, the macro-FEM analysis provides stiff assembly as well as u_z^{macro} displacements, assuming perfect components without geometric defects as shown in Fig.5. The corresponding displacement results are illustrated in Fig.6, showing the response for the first 150 selected nodes. These results serve as input for the subsequent analysis using the MDR method.

2.2 PINN (MDR) model

PINNs are applied across various fields, including fluid, thermal, structural, and contact mechanics [11,12], and are increasingly regarded as a new class of numerical solvers for PDEs, aiming to approximate their solutions directly [13,14]. A PINN neural network, characterized by its parameters θ and the radial coordinates r of the displacement, is defined by (6):

$$\hat{w} = \mathcal{N}_w(\theta, r) \tag{6}$$

When considering the normal displacement $w_{MDR}(r, a)$ over two zones:

- For $r < a$ inside the contact zone,
- For $r > a$ outside the contact zone,

Thus, it is necessary to define two distinct neural networks, each one to reproduce the approximate solution on one of the two areas by (7) and (8):

$$\hat{w}_{in} = \mathcal{N}_w^{in}(\theta, r) \tag{7}$$

$$\hat{w}_{out} = \mathcal{N}_w^{out}(\theta, r) \tag{8}$$

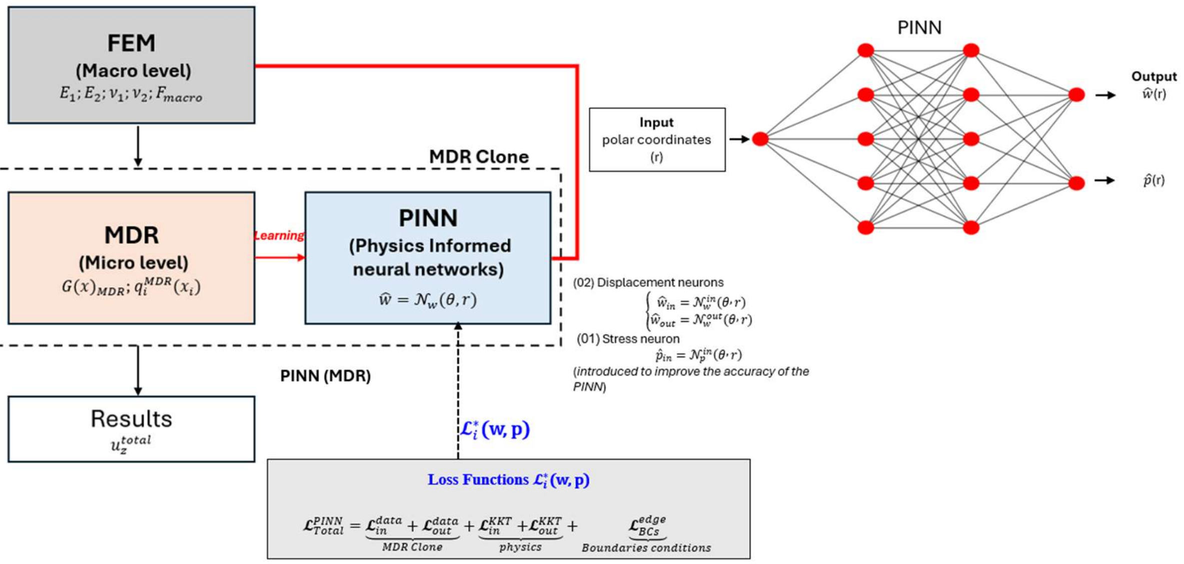

Fig.7 Physics-informed neural network as an MDR clone

by recalling the physical laws used for training PINNs based on the exact solutions of the MDR.

For frictionless normal contact, these laws and constraints are formalized as follows:

For global equilibrium, the normal force is written as in (9):

$$F_N = 2E^* \int_0^a [d - G(x)]\, dx \qquad (9)$$

According to the Karush–Kuhn–Tucker (KKT) contact law, the contact conditions can be expressed as follows by (10):

$$g(r) = (d - G_{MDR}(\mathrm{x})) - w(r) \leq 0 \qquad (10)$$

And then the condition of non-penetration can be written by (11):

$$\begin{cases} g(r) \leq 0; \\ p(r) \geq 0 \\ g(r)\, p(r) = 0 \end{cases} \qquad (11)$$

Then for r < a, g(r)=0; the two surfaces of the plate are in contact p(r)>0. On the contrary for r>a, g(r)<0; the two surfaces are separated; p(r)=0.

The micro-displacements obtained from the MRD are superimposed onto the macro-displacements $u_z^{macro}(x_i)$ computed using FEM. This allows the evaluation of the total displacement as well as the final pressure distribution $q_i^{MRD}(x)$, in accordance with (12):

$$u_z^{total}(x_i) = u_z^{macro}(x_i) + u_z^{micro}(x_i), \text{with } u_z^{micro}(x_i) = w(x_i) - d_{max} \qquad (12)$$

As illustrated in Fig.7, the exact response of the MDR method will be used in PINN neural network. The training therefore consists of adjusting the network parameters to minimize this difference, ensuring that the model faithfully reproduces the deformation and contact behaviors obtained from the analytical method.

The main loss functions defined in this work are formulated as follows:

Data loss IN and Out of the contact zone are given by (13) and (14):

$$\mathcal{L}_{in}^{data} = \frac{1}{N_{in}} \sum_{j=1}^{N_{in}} ([\hat{p}_{in}(r_i) - p_{MDR}(r_i)]^2 + \alpha_w [\widehat{w}_{in}(r_i) - w_{MDR}(r_i)]^2) \qquad (13)$$

$$\mathcal{L}_{out}^{data} = \frac{1}{N_{out}} \sum_{j=1}^{N_{out}} ([\widehat{w}_{out}(r_i) - w_{MDR}(r_i)]^2) \qquad (14)$$

The integration of the neuron $\hat{p}_{in} = \mathcal{N}_p^{in}(\theta, r)$ aims to enhance the performance of the PINN.

KKT (contact/non-contact) losses are given by (15) and (16):

$$\mathcal{L}_{in}^{KKT} = \frac{1}{N_{in}} \sum_{j=1}^{N_{in}} \left(g_{in}(r_i)^2 + \beta_p \, ReLU\,(-\hat{p}_{in}(r_i))^2 \right) \quad (15)$$

$$\mathcal{L}_{out}^{KKT} = \frac{1}{N_{out}} \sum_{j=1}^{N_{out}} \left(\beta_g \, ReLU\,(-\hat{g}_{out}(r_i))^2 \right) \quad (16)$$

Loss of balance is given by (17):

$$\mathcal{L}_{equilibrium}^{Force} = (\hat{F}_N - F_N^{(MDR)}) \quad (17)$$

Loss at edge conditions is defined by (18):

For $r = a_{MDR}$;

$$\mathcal{L}_{BCs}^{edge} = \gamma_p \hat{p}_{in}(a_{MDR})^2 + \gamma_c (\hat{w}_{in}(a_{MDR}) - \hat{w}_{out}(a_{MDR}))^2 \quad (18)$$

Total Loss is given by (19):

$$\mathcal{L}_{Total}^{PINN} = \underbrace{\mathcal{L}_{in}^{data} + \mathcal{L}_{out}^{data}}_{MDR\ Clone} + \underbrace{\mathcal{L}_{in}^{KKT} + \mathcal{L}_{out}^{KKT}}_{physics} + \underbrace{\mathcal{L}_{BCs}^{edge}}_{Boundaries\ conditions} \quad (19)$$

Where the parameters $\alpha_w; \beta_p; \beta_g; \gamma_p \; et \; \gamma_c$ are weights of regularization.

3. Results and discussions

From a geometric variation standpoint, for a maximum deviation $d_{max} = 0.38$ mm and a micro-defect amplitude $A = 5\,\mu$m, the normal micro-displacement induced by surface roughness is on the order of $u_z^{micro} \sim A = 5\,\mu$m. This contribution represents approximately 1.3% of the overall assembly deviation, and therefore remains very small.

The physics-informed neural network (PINN) is able to accurately predict the solutions when compared to the MDR results. Fig.8 presents the PINN predictions (blue solid line) alongside the MDR (red dashed line) solutions and showing excellent agreement. The application of PINNs is particularly advantageous, as it enables the evaluation of micro-defects in a meshless framework while reducing computational cost and maintaining solution accuracy. This differs from classical approaches reported in literature and based solely on full 3D FEM simulations [2], which require mesh refinement and therefore result in a large number of elements and high computational cost.

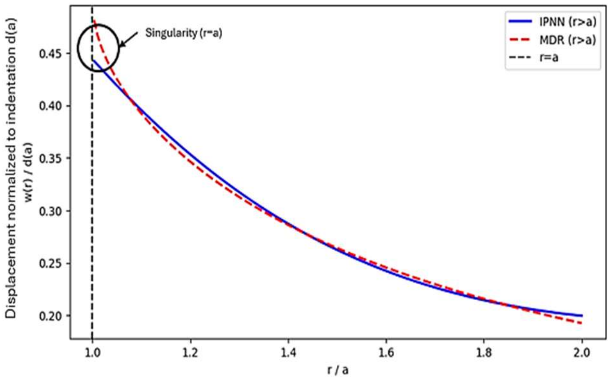

Fig.8 Result of PINN prediction (blue solid line) showing the displacement normilazed to the indentation d(a)

The main advantages and potential limitations of the proposed FEM–PINN (MDR) model are summarized in Table1, highlighting its computational efficiency, capability to capture micro-defects associated with assumptions.

Table 1 Advantages and limitations of the proposed FEM–PINN (MDR) Model

	Advantages	Disadvantages
FEM-PINN (MDR) model	- Complexity reduced (1D). -Calculation Time reduced compared to full 3D FEM simulations. - Enables efficient detection of micro-defects through the coupling of FEM macro-analysis and PINN micro-analysis.	-Singularity can be presented in the solution. - Highly dependent on the adjustment of the neural network hyperparameters.

The model also has some limitations. The accuracy of PINN is highly dependent on the selection and tuning of neural network hyperparameters, such as the number of layers, learning rate, and activation functions. Additionally, due to the reduced dimensionality of the model, localized singularities may occur, resulting in slight deviations near contact edges.

4. Conclusion

In this work, a hybrid FEM–PINN (MDR) model is presented for predicting assembly variations while accounting for micro-geometric defects.

The results demonstrate that the proposed approach accurately captures the influence of small-scale defects on the overall assembly behavior. By coupling physics-based modeling with data-driven learning, the methodology achieves a balance between computational efficiency and solution fidelity. The study confirms the effectiveness of integrating reduced-dimensionality methods and physics-informed neural networks for mechanical assembly analysis, offering a robust and practical tool for improving the precision and reliability of engineering designs.

References

[1] M. Ghali, S. Elghali, N. Aifaoui, Associated tolerance optimization approach using manufacturing difficulty coefficients and genetic algorithm, Assembly Automation 6 December, 42 (6) (2022) 782–795.

[2] C. Lacroix, Caractérisation géométrique des assemblages flexibles par la mesure, Ecole normale supérieure de Cachan-ENS Cachan, France, 2015.

[3] A. Stricher, Tolérancement flexible d'assemblages de grandes structures aéronautiques, Ph.D Thesis, Ecole Normale Supérieure de Cachan-ENS, France, 2013.

[4] H. Atik, M. Chahbouni, D. Amegouz, S. Boutahari, A new tolerance analysis approach for deformable assemblies: an industrial case study, International Journal of Engineering and Technology 11, (2019) 594–605.

[5] A. Radhouan, M. Ghali, N. Aifaoui, Tolerance Analysis for the Assembly of Non-rigid Parts with Form Defects, In: M. Chouchane et al., Design and Modeling of Mechanical Systems-VI, CMSM 2023, Lecture Notes in Mechanical Engineering, Springer, Cham (2024).

[6] J. Kenneth Langstreth, Contact mechanics, Cambridge University Press, 1987.

[7] H. Ben Dhia, C. Zammali, Level-Sets and Arlequin framework for dynamic contact problems, Revue Européenne des éléments finis, 13, 5,6,7, (2004) 403-414.

[8] V. Popov, M. Heß, Method of dimensionality reduction in contact mechanics and friction, Springer, Heidelberg (2015).

[9] P. Wriggers, O. Scherf, C. Carstensen, C, Adaptive techniques for the contact of elastic bodies, In J. Hughes, E. Onate and O. Zienkiewicz, editors, Recent Developments in Finite Element Analysis, CIMNE, Barcelona, (1994) 78–86.

[10] A. Radhouan, M. Ghali, N. Aifaoui, A mathematical formulation for predicting the deviation of flexible assemblies based on the dimensionality reduction method, Int J Interact Des Manuf, (2025).

[11] K. Luo, J. Zhao, Y. Wang et al., Physics-informed neural networks for PDE problems: a comprehensive review, Artif Intell Rev 58, (2025) 323.

[12] W. Peng, J. Zhang, W. Zhou, X. Zhao, W. Yao, X. Chen IDRLNet: A physics-informed neural network library, 2021.

[13] M. Raissi, P. Perdikaris, G. Karniadakis, Physics-informed neural networks: A deep learning framework for solving forward and inverse problems involving nonlinear partial differential equations, Journal of Computational Physics, 378, (2019) 686–707.

[14] T. Sahin, M. von Danwitz, A. Popp, Solving forward and inverse problems of contact mechanics using physics-informed neural networks, Advanced Modeling and Simulation in Engineering Sciences, 11, 11 (2024).